# Dynamic Downlink Power Control Strategies for LTE Femtocells

Xiang Xu, Gledi Kutrolli and Rudolf Mathar
Institute for Theoretical Information Technology, RWTH Aachen University
Aachen, Germany 52074
Email: {xu,kutrolli,mathar}@ti.rwth-aachen.de

***Abstract*—In this work, dynamic downlink power control schemes based on user type identification are proposed for LTE (Long Term Evolution) femtocells. In the proposed schemes, the users are distinguished by their serving cells and service types, and the power control is performed accordingly. Moreover, with a variable setting of data rate offset, the proposed schemes can achieve superior performance in terms of a well-balanced data throughput and coverage.**

***Index Terms*—Power control, femtocell, LTE, channel quality indicator**

## I. Introduction

As one of the important features of LTE, femtocell is developed to overcome the indoor coverage problem [1]. Small base stations, known as HeNBs (Home evolved Node B) in LTE terminology, are deployed in femtocells. HeNBs generally have a maximum transmit (Tx) power of 10-20 dBm, which results in a covered range of 10-30 meters. Due the shield of electro-magnetic wave caused by building walls, HeNBs are supposed to have limited interference to the outdoor users, while giving the indoor users a seamless mobile connection.

HeNBs utilize the existing wired infrastructure to connect to the backbone network, thus can be deployed in large scale. The initial configuration and later operation of the HeNB should be in a self-organized manner, such that the mobile users do not need experts to help them to deploy femtocells at home or in the offices. The plug and play nature of HeNBs leads to many restrictions on designing the management algorithms. Unlike the eNBs, which are in fixed locations and always online, HeNBs can be moved from one room to another, or be turned on and off randomly. Algorithms which use static location information become infeasible, and autonomous management algorithms are demanded [2].

HeNBs can either share the spectrum with the macro base station, which is called eNBs (evolved Node B) in LTE terms, or use a dedicated channel. Although the dedicated channel deployment avoids the problem of co-channel interference (CCI), both eNBs and HeNBs can only have a part of the available spectrum, thus have smaller bandwidth and possibly lower data throughput [3]. Due to this reason, partial sharing of the spectrum is usually preferred, where the eNBs can use the full available frequency band and HeNBs can use only a part of it. The overlapped frequency band leads to CCI, which should be mitigated by using radio resource allocation and Tx power control.

This work is partially supported by UMIC, a research project in the frame work of the German excellence initiative.

In previous works, the power control algorithms are usually based on the signal to interference plus noise ratio (SINR) [4]. However, in LTE systems, the downlink SINR level is typically unavailable at the base station. Instead, 3GPP LTE standards specify a highly quantized channel quality indicator (CQI), which is send from UEs to eNBs or HeNBs, as an indication of the channel quality. Actually, the quantized CQI results in a finite solution set, thus makes the power control problem easier to solve. The method proposed in this work heavily depends on the CQI feedback mechanism. Furthermore, power control schemes for the overlayed macrocell and femtocell often come with strong assumptions. In [3], the full knowledge of the network layout is a prerequisite. Two methods proposed in [5] guaranties the indoor home-UE (HUE) to have at least the same received power as if it is an outdoor macro-UE (MUE). However, those two methods either demands a large amount of information, such as cell locations, power levels, antenna orientations and gains etc. or assumes a perfect feedback channel. The scheme mentioned in [6] utilizes additional uplink receive (Rx) power from MUE to improve performance, but it has similar drawbacks as aforementioned. In [7], a centralized solution with the assumption of perfect coordination among eNBs and HeNBs is suggested.

Another issue of the existing methods is, the service type of UE is not taken into account. Since different services have different data rate demands, using small Tx power for low demand services would significantly reduce the interference to the other UEs without sacrificing the throughput or coverage.

The main contribution of this work is a fully decentralized, self-organized heuristic for the downlink power control and interference mitigation in LTE femtocells. The proposed power control schemes dynamically adjust the Tx power to adapt to the UE types and quality of service (QoS) requirements. No strong assumptions, such as the knowledge of the whole network or location of every UE, are needed by the proposed scheme. Additionally, according to the network environment, HeNBs can update their settings to further improve the performance. The proposed scheme is able to produce a considerable performance gain in Monte-Carlo simulations.

978-0-7695-5090-9/13 $26.00 © 2013 IEEE
DOI 10.1109/NGMAST.2013.40

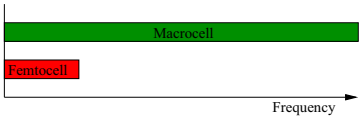


Fig. 1. Partial frequency sharing.

## II. Preliminaries

### A. Femtocell deployments

The deployments of femtocells can be categorized in two ways, namely, according to the spectrum allocation and access mode.

As mentioned before, the femtocells can use a dedicated channel, or, to efficiently use the spectrum resources, HeNBs can use overlapped spectrum with eNBs. Due to the small coverage of the HeNB, it is not likely for a HeNB to serve many UEs. Thus, the HeNB can use only a part of the available frequency band to avoid CCI. The partial sharing scheme also enables smart resource allocation in eNBs, where their exclusive part of the spectrum can be allocated firstly [2]. Furthermore, HeNBs can use different part of the frequency to avoid interfering each other. However, coordination among neighboring HeNBs will be needed. In this work, the partial sharing illustrated in Fig. 1 is considered.

According to the access mode, femtocells can be divided into open access and closed subscriber group (CSG). All the UEs, which are close enough to a HeNB, can be handed over to the HeNB in open access mode, whereas only the licensed UEs can be served in the CSG mode. In CSG mode, the unlicensed MUE can potentially suffer from strong interference from the nearby HeNBs. From commercial point of view, since the femtocells are intended to be deployed by the end users, who pay for the HeNB to boost the signal strength on their own devices, it is unlikely that they would use the open access mode. Due to this reason, only CSG is considered in this work.

### B. System model

The cellular system is mostly interference limited, which means the SINR calculation relies on identifying the interference sources. The CCIs for different UEs are illustrated in Fig. 2. Consider a cellular network with $M$ macrocells, a MUE $v$ served by eNB $m$ is interfered by the other $M-1$ eNBs. In addition, if it is close to HeNBs, the HeNBs are also the source of interference. The SINR of MUE $v$ can be written as

$$\gamma_v = \frac{P_{m,v}^{(\mathrm{MC})}}{\sum_{i=1,i\neq m}^{M} P_{i,v}^{(\mathrm{MC})} + \sum_{j=1}^{F} P_{j,v}^{(\mathrm{FC})} + N_v}, \tag{1}$$

where $P_{m,v}^{(\mathrm{MC})}$, $P_{i,v}^{(\mathrm{MC})}$, $P_{j,v}^{(\mathrm{FC})}$ are the Rx power from the serving macrocell, interfering macrocells and interfering femtocell, respectively. $N$ is the thermal noise power. $F$ is the number of interfering femtocells.

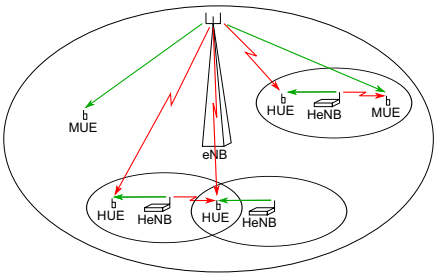


Fig. 2. Co-channel interferences in overlayed macrocell and femtocell deployment.

The SINR of a HUE $u$ can be calculated in a similar way

$$\gamma_u = \frac{P_{f,u}^{(\mathrm{FC})}}{\sum_{i=1}^{M} P_{i,u}^{(\mathrm{MC})} + \sum_{j=1,j\neq f}^{F} P_{j,u}^{(\mathrm{FC})} + N_u}. \tag{2}$$

The term $P_{j,u}^{(\mathrm{FC})}$ represents inter-femtocell interference, which is likely to exist when the femtocells are densely located. Although the power and noise are typically changing over time, for the sake of simplicity, time indices are omitted here, and the formulas are valid for a snapshot.

The Rx power on UE side is contributed by several parts, including the Tx power, Tx antenna gain, pathloss and fading. Taking MUE as example, macrocell Rx power $P_{i,u}^{(\mathrm{MC})}$ can be calculated by

$$P_{i,u}^{(\mathrm{MC})} = \frac{P_{\mathrm{Tx},i}^{(\mathrm{MC})} G_{\mathrm{Tx},i}^{(\mathrm{MC})} H_{i,u}^{(\mathrm{MC})}}{L_{i,u}^{(\mathrm{MC})}}, \tag{3}$$

where $P_{\mathrm{Tx},i}^{(\mathrm{MC})}$ and $G_{\mathrm{Tx},i}^{(\mathrm{MC})}$ are the Tx power and antenna gain of the $i$th eNB, $H_{i,u}^{(\mathrm{MC})}$ and $L_{i,u}^{(\mathrm{MC})}$ are the normalized channel gain and pathloss of the wireless link between the $i$th eNB and $u$th UE, respectively. The Rx power of femtocell $P_{f,u}^{(\mathrm{FC})}$ can be calculated in the same way.

The pathloss is usually modeled empirically. The general form of the pathloss is

$$L_{i,u} = A + B \log r_{i,u}, \tag{4}$$

where $r_{i,u}$ is the distance between $i$th eNB and $u$th UE, $A$ and $B$ are empirically calibrated parameters. Due to the existence of buildings, as depicted in Fig. 3, an extra wall penetration loss should be applied.

### C. Channel quality indicator

To reduce the signaling overhead, LTE specifies the 4-bit CQI as an indicator of the SINR [8]. The SINR is measured at the UE, and compressed into this 4-bit CQI and sent back to the base station [9]. As shown in Tab. I, each CQI value corresponds to an unique modulation and coding scheme (MCS), so that the eNB or HeNB can use high-order modulation and high coding rate for high spectral efficiency in channels with high SINR, or, low-order modulation and low

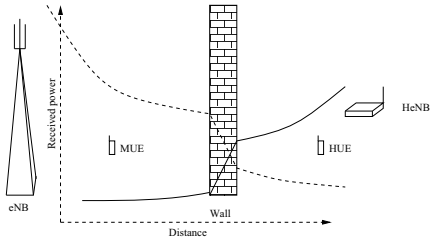


Fig. 3. Pathloss and extra wall penetration loss.

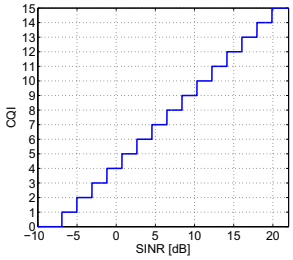


Fig. 4. Mapping from SINR to CQI.

coding rate for good error protection in channels with low SINR.

The CQI is chosen as the input of the proposed algorithm for two reasons. Firstly, in current LTE standards, it is not possible to get more accurate information about the downlink SINR other than using the CQI. Secondly, instead of a continuous variable of SINR, CQI is discrete and has a relatively small cardinality, which can significantly simplify the optimization process. In this work, CQI is modeled as a linear step function of SINR, where the step size of SINR defined as $\Delta P_{\mathrm{Tx,CQI}}$ can be obtained by extensive simulations, as shown in Fig. 4 [10]. It is also assumed that CQI values are accurate and available for each subcarrier.

### D. Service types

The services of the users have different priorities, data rate and QoS requirements, and accordingly, they are modeled into three different classes, as shown in Tab. II. VoIP service has the highest priority and a fixed data rate of 64 kpbs. It is margin adaptive (MA), as the Tx power should be minimized, while the data rate requirements are satisfied. The data service has a medium priority and a fixed data rate between 512 kbps and 2000 kbps. The web service has the lowest priority and it is rate adaptive (RA). That means if the data rate meets the lowest requirement, the UE is satisfied, however, the data rate should be maximized subject to the power limit [12]. The percentage of UEs using each service is also given in Tab. II.

| CQI index | Modulation | Code rate × 1024 | Efficiency [bit/s/Hz] |
|---|---|---|---|
| 0 | out of range | | |
| 1 | QPSK | 78 | 0.1523 |
| 2 | QPSK | 120 | 0.2344 |
| 3 | QPSK | 193 | 0.3770 |
| 4 | QPSK | 308 | 0.6016 |
| 5 | QPSK | 449 | 0.8770 |
| 6 | QPSK | 602 | 1.1758 |
| 7 | 16QAM | 378 | 1.4766 |
| 8 | 16QAM | 490 | 1.9141 |
| 9 | 16QAM | 616 | 2.4063 |
| 10 | 64QAM | 466 | 2.7305 |
| 11 | 64QAM | 567 | 3.3223 |
| 12 | 64QAM | 666 | 3.9023 |
| 13 | 64QAM | 772 | 4.5234 |
| 14 | 64QAM | 873 | 5.1152 |
| 15 | 64QAM | 948 | 5.5547 |

TABLE I
THE 4-BIT CQI TABLE IN LTE [11]

### E. Resource allocation

A decentralized resource allocation scheme is adopted for both eNB and HeNB. The base station first sorts its associated UEs according to their priorities. Following this order, one by one, the UEs pick the physical resource block (PRB) with highest CQIs, until their data rate requirements are fulfilled. After that, the rest of the radio resources are assigned to the web users. In this procedure, each eNB or HeNB makes their own decision, regardless the assignment of the others.

## III. Power Control Schemes

### A. Power control with fixed data rate offset

The central idea of the dynamic power control algorithms is to gradually raise the Tx power from its minimum until the exact amount of the power which can satisfy all the HUEs is used [13]. In this sense, the QoS is guaranteed without causing too much interference to the other UEs. For MA users, it is rather straight forward, the target throughput is the minimum throughput requirement $T^{(\mathrm{FC})}_{\mathrm{target},u} = T^{(\mathrm{FC})}_{\mathrm{min},u}$. However, it is more difficult to deal with RA users, since the data rate should be maximized subject to the power limit. A simple heuristic is to set a data rate offset $\alpha \geq 0$ Mbps for the web users, such that the web users can have an incremental throughput of $\alpha$. So the data rate requirement for web UE becomes $T^{(\mathrm{FC})}_{\mathrm{target},u} = T^{(\mathrm{FC})}_{\mathrm{min},u} + \alpha$. With $\alpha = 0$ Mbps, the web users will have only the minimum data rate, whereas with $\alpha \to \infty$ Mbps, the web users are really rate adaptive.

As illustrated in Algorithm 1, the HeNB first set its Tx power to the minimum $P^{(FC)}_{\mathrm{Tx,min}}$, and then calculate the target throughput $T^{(\mathrm{FC})}_{\mathrm{target}}$ which is the summation of data rate demand of all the HUEs served by this HeNB. After that, for each HUE, its required number of PRBs is calculated with proportion of the individual throughput requirement to the overall throughput requirement in that femtocell. The $\lceil \cdot \rceil$ operator makes sure that each UE get at least one PRB. The throughput target and number of PRBs can be translated into

| Service | Priority | Data rate $T_{\mathrm{min},u}$ | Type | Percentage |
|---|---|---|---|---|
| VoIP | High | 64 kbps | MA | 10% |
| Data | Mid | [512-2000] kbps | MA | 40% |
| Web | Low | $\geq$ 64 kbps | RA | 50% |

TABLE II
DIFFERENT TYPES OF SERVICE

**Algorithm 1** Power control algorithm with fixed $\alpha$

**for all** HeNB **do**
  **function** SETPOWER($\alpha$)
    $P_{\mathrm{Tx,CQI}}^{(FC)} \leftarrow P_{\mathrm{Tx,min}}^{(FC)}$
    $T_{\mathrm{target}}^{(\mathrm{FC})} \leftarrow \sum_{u=1}^{N_{\mathrm{UE}}^{(\mathrm{FC})}} T_{\mathrm{target},u}^{(\mathrm{FC})}$
    **for all** HUE **do**
      $N_{\mathrm{PRB},u}^{(\mathrm{FC})} \leftarrow \lceil \frac{T_{\mathrm{target},u}^{(\mathrm{FC})}}{T_{\mathrm{target}}^{(\mathrm{FC})}} \cdot (N_{\mathrm{PRB}}^{(\mathrm{FC})} - N_{\mathrm{UE}}^{(\mathrm{FC})} + 1) \rceil$
      $R \leftarrow \lceil g(\frac{T_{\mathrm{target},u}^{(\mathrm{FC})}}{N_{\mathrm{PRB},u}^{(\mathrm{FC})}}) \rceil$
      **while** $Q < R$ && $P_{\mathrm{Tx,CQI}}^{(FC)} < P_{\mathrm{Tx,max}}^{(FC)}$ **do**
        $P_{\mathrm{Tx,CQI}}^{(FC)} \leftarrow P_{\mathrm{Tx,CQI}}^{(FC)} + \Delta P_{\mathrm{Tx}}$
      **end while**
    **end for**
  **end function**
**end for**

the spectral efficiency. And the target CQI is calculated, using the spectral efficiency to CQI mapping function $g(\cdot)$, which can be obtained from Tab. I. For each HUE, the power will keep rising with a granularity of $\Delta P_{\mathrm{Tx}}$ until the actual CQI $Q$ is greater than or equal to the target CQI $R$, or the Tx power reaches its maximum. The value of $\Delta P_{\mathrm{Tx}}$ determines how fast this algorithm converges. Since the CQI is always an integer, one can find that it changes value only if the variation in SINR is large than its step size $\Delta P_{\mathrm{Tx,CQI}}$ by observing Fig. 4. Considering multiple close-by femtocells can influence each other, $\Delta P_{\mathrm{Tx}} = \Delta P_{\mathrm{Tx,CQI}}/2$ in this work.

### B. Power control with variable data rate offset

The selection of $\alpha$ is greatly important for this power control algorithm. Generally speaking, there is a trade-off between throughput and coverage. Larger $\alpha$ leads to a higher throughput for the HUEs but potentially lower overall coverage, due to the large interference to the MUEs. Although $\alpha \to \infty$ Mbps always results in a target CQI $R = 15$, it is not equivalent to using maximum Tx power, because the algorithm stops at the point where the actual CQI $Q$ reaches $R$.

Other than using a predetermined value for all the HeNBs, $\alpha$ can also be tuned as a variable. In this case, HeNB listen to the uplink channel and detect how many UEs are within its covered range [14], and adjust its Tx power accordingly. Since the HUEs are generally close to the HeNBs and have strong signals, while the MUEs close to the HeNBs are most vulnerable, $\alpha$ will be set to 0 if any MUE presents. Otherwise, a heuristic $\alpha = \beta^{1-N_{\mathrm{HUE}}}$ is applied in this work, where $N_{\mathrm{HUE}}$ is the number of interfered HUEs in the covered area and $\beta$ is a control parameter. As the number of interfered HUEs increases, $\alpha$ decreases exponentially to avoid interference. In this sense, a well balanced coverage and throughput can be achieved by using the variable settings. This process is done prior to the actual power control algorithm, as summarized in Algorithm 2.

**Algorithm 2** Power control algorithm with variable $\alpha$

**for all** HeNB **do**
  **if** exist UE in range **then**
    **if** exist MUE in range **then**
      $\alpha \leftarrow 0$
    **else**
      $\alpha \leftarrow \beta^{1-N_{\mathrm{HUE}}}$
    **end if**
  **else**
    $\alpha \leftarrow \infty$
  **end if**
  SETPOWER($\alpha$)
**end for**

| | HeNB | eNB |
|---|---|---|
| Carrier frequency | 2 GHz | 2GHz |
| Spectrum | 1 MHz | 10 MHz |
| Antenna pattern | Omni-directional | 3-sector |
| Max. Tx power | 20 dBm | 46 dBm |
| Antenna gain | 5 dBi | 14 dBi |

TABLE III
SIMULATION PARAMETERS.

## IV. SIMULATION RESULTS

### A. Simulation environment

As shown in Fig. 5 (a), the simulation is conducted for an urban area with 19 eNBs, each serving 3 cells. The inter-site distance is 500 meters. Multiple buildings are randomly located in the simulated area. On average, each cell has one building with 40 apartments. The apartments are located in dual-stripe blocks as shown in Fig. 5 (b) [15]. 20% percent of the randomly chosen apartments are equipped with HeNBs in the middle of the rooms. The activation rate of HeNBs is 50%. The penetration loss is $L_{\mathrm{iw}} = 5$ dB for the inner wall and $L_{\mathrm{ow}} = 10$ dB for the outer wall. Some other parameters of the eNB and HeNB are summarized in Tab. III.

In total 400 MUEs are simulated, with 80% of them located indoor. In addition, each HeNB serves 2 HUEs, which are in the same apartment. Mobility models are employed to create realistic movement patterns of the UEs. The indoor UEs can move freely inside the apartments and outdoor UEs can only move along some streets, which are laid orthogonally over the map. The mobility parameters are given in Tab. IV.

The channel gain $H$ is modeled as Rayleigh process using autoregressive filtering [16], and the pathloss $L$ is modeled as described in Tab. V, where $r$ is the distance between base station and UE, $d$ is the distance between the UE and its projection on the building wall, $q$ is the number of inner walls separating base station and UE.

| User | Average speed | Mobility pattern |
|---|---|---|
| Outdoor pedestrian | 1 m/s | Along streets |
| Outdoor vehicular | 10 m/s | Along streets |
| Indoor pedestrian | 1 m/s | Indoor, random |

TABLE IV
USER MOBILITY PARAMETERS.

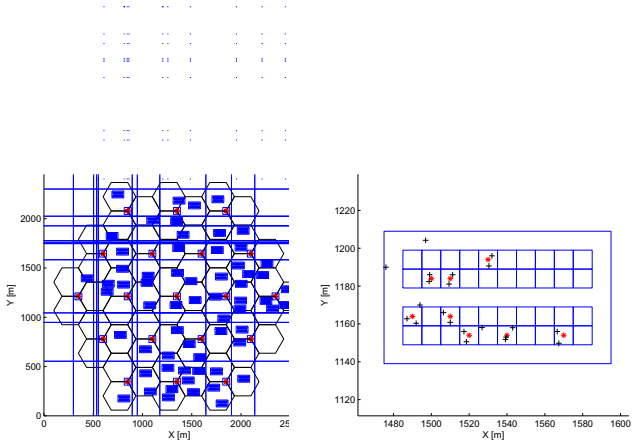


(a) (b)

Fig. 5. (a) Simulation environment, horizontal and vertical lines represent streets, "$*$"s are eNBs and rectangles are building blocks. (b) Dual-stripe building model with red $*$'s as HeNBs and black +'s as UEs

### B. Metrics and references

In the simulation, the performance is measured for coverage and throughput. Coverage is defined by the overall satisfaction rate of all the UEs. An UE is satisfied, whenever its lowest data rate requirement is met. The calculation of throughput differs from margin adaptive UE to rate adaptive UE. Unlike the calculation using Shannon's formula, a margin adaptive UE cannot have throughput higher than it demands, even if its Rx power can provide such throughput. A rate adaptive UE can get its maximum achievable throughput according to its channel quality.

The following schemes are considered for evaluation: (1). Without power control, all the HeNBs transmit with maximum power. (2). The measurement-based power control from [5]. (3). The dynamic power control scheme with different settings of $\alpha$. (4). The dynamic power control with the variable setting of $\alpha$. The control parameter $\beta$ is set to 5.

The measurement-based power control is a conventional method, which aims at providing the HUE in a radius $r_{\max}$ at least the same amount of Rx power from the strongest macrocell signal. The Tx power of the measurement-based scheme is

$$P_{\text{Tx,meas}}^{(\text{FC})} \triangleq \min(P_{m,f}^{(\text{MC})} L_f^{(\text{FC})}(r_{\max}), P_{\text{Tx,max}}^{(\text{FC})}), \qquad (5)$$

where $P_{m,f}^{(\text{MC})}$ is the measured macrocell downlink Rx power at the location of HeNB, $L_f^{(\text{FC})}$ is the femtocell pathloss.

| | |
|---|---|
| eNB-indoor UE | $L_{m,u,\text{dB}}^{(\text{MC})} = 15.3 + 37.6 \log r_{m,u} + q \cdot L_{\text{iw}} + L_{\text{ow}}$ |
| eNB-outdoor UE | $L_{m,v,\text{dB}}^{(\text{MC})} = 15.3 + 37.6 \log r_{m,v}$ |
| HeNB-indoor UE | $L_{f,v,\text{dB}}^{(\text{FC})} = \max(38.46 + 20 \log r_{f,v}, 15.3 + 37.6 \log r_{f,v}) + 0.7 d_{f,v} + q \cdot L_{\text{iw}}$ |
| HeNB-outdoor UE | $L_{f,v,\text{dB}}^{(\text{FC})} = \max(38.46 + 20 \log r_{f,v}, 15.3 + 37.6 \log r_{f,v}) + 0.7 d_{f,v} + q \cdot L_{\text{iw}} + L_{\text{ow}}$ |

TABLE V
PATHLOSS MODELS.

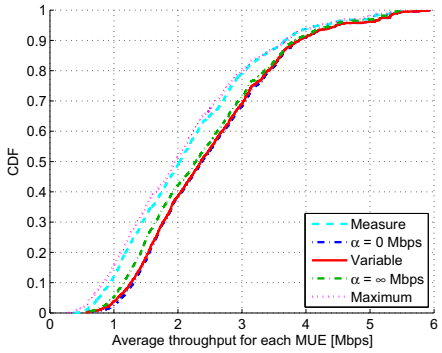


Fig. 6. Throughput CDF of MUEs

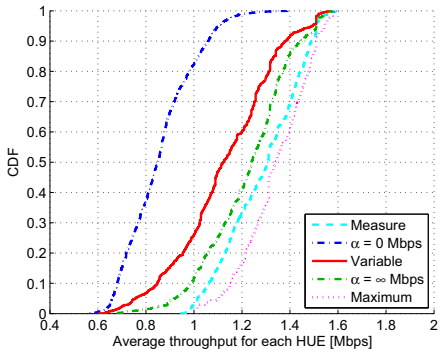


Fig. 7. Throughput CDF of HUEs

### C. Numerical results

The throughput cumulative density functions (CDF) are compared for MUEs, HUEs and all UEs, respectively. For MUEs, the measurement-based scheme (denoted as "Measure") and maximum Tx power have similar bad performance, while due to the reduction of interference, the dynamic schemes perform considerably better. Fixed $\alpha = 0$ Mbps and variable $\alpha$ have the best throughput at the same time, as depicted in Fig. 6.

The reduction of interference comes at the price of lower signal power for the HUEs. As shown in Fig. 7, using maximum power gives the best performance for HUEs. All of the proposed power control schemes have lower throughput than the measurement based scheme and the maximum power scheme. Especially for $\alpha = 0$ Mbps, as given in Fig. 8, the penalty for HUEs eventually leads to an evident gap in overall throughput comparing to the other schemes, which all have similar throughput.

The overall throughput is compared in Fig. 9, where the measurement-based scheme performs almost the same as using maximum power. The scheme with variable $\alpha$ has better throughput. Furthermore, the throughput for the fixed $\alpha$ is almost monotonically increasing and only advantageous when

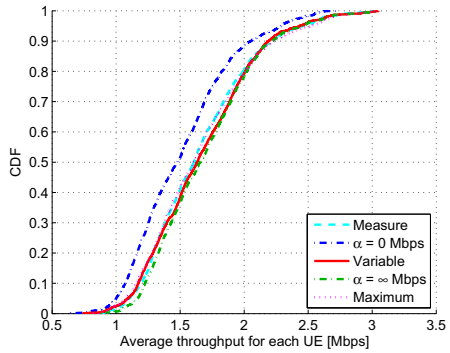


Fig. 8. Throughput CDF of all UEs

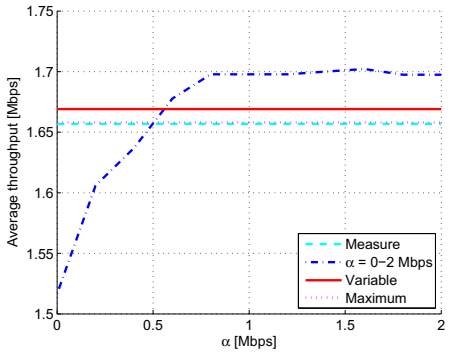


Fig. 9. Average throughput for different schemes

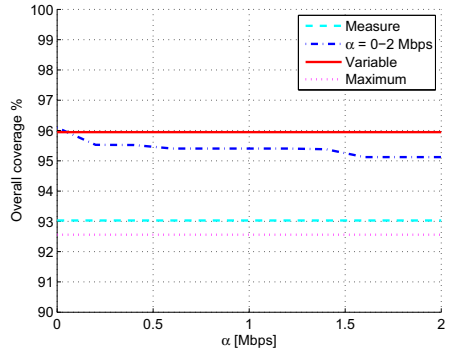


Fig. 10. Average coverage for different schemes

$\alpha$ is large.

Judging from the throughput, the proposed power control scheme with variable $\alpha$ has an advantage over the measurement based scheme and maximum power. Furthermore, there is always a trade off between throughput and coverage, and from the operator's point of view, coverage is usually more important than throughput [2]. The overall coverage of the selected schemes are compared in Fig. 10. The overall coverage decreases as the value of $\alpha$ increases in the dynamic scheme with fixed $\alpha$. The scheme with $\alpha = 0$ Mbps delivers superior performance. And the scheme with variable $\alpha$ has almost no performance loss comparing to $\alpha = 0$ Mbps. Meanwhile, it offers more than 10% gain in average throughput. In this context, the advantage of using the dynamic scheme with variable $\alpha$ is clear.

## V. Conclusion

In this work, simple, decentralized, dynamic power control schemes are presented. The proposed schemes consider different QoS requirements for different services. The interference to MUEs can be suppressed, without degradation of the performance of HUEs. Without strong assumptions, the proposed schemes can be easily implemented. In the simulation, using a variable data rate offset shows almost the best coverage and higher throughput than the scheme with similar coverage.

## References

[1] Motorola, "Femtocells - the gateway to the home," White paper, 2008.
[2] A. Engels, M. Reyer, X. Xu, R. Mathar, J. Zhang, and H. Zhuang, "Autonomous self-optimization of coverage and capacity in LTE cellular networks," *IEEE Transactions on Vehicular Technology, Special Issue: Self-Organizing Radio Networks*, vol. 62, no. 5, pp. 1989–2004, 2013.
[3] H. Mahmoud and I. Guvenc, "A comparative study of different deployment modes for femtocell networks," in *Personal, Indoor and Mobile Radio Communications, IEEE 20th International Symposium on (PIMRC)*, Tokyo, Japan, Sep. 2009.
[4] V. Chandrasekhar, J. Andrews, T. Muharemovict, Z. Shen, and A. Gatherer, "Power control in two-tier femtocell networks," *Wireless Communications, IEEE Transactions on*, vol. 8, no. 8, pp. 4316–4328, 2009.
[5] H. Claussen, L. T. W. Ho, and L. G. Samuel, "Self-optimization of coverage for femtocell deployments," in *Wireless Telecommunications Symposium, (WTS)*, Pomona, USA, Apr. 2008.
[6] M. Morita, Y. Matsunaga, and K. Hamabe, "Adaptive power level setting of femtocell base stations for mitigating interference with macrocells," in *Vehicular Technology Conference Fall (VTC Fall), IEEE 72nd*, Ottawa, Canada, Sep. 2010.
[7] X. Li, L. Qian, and D. Kataria, "Downlink power control in co-channel macrocell femtocell overlay," in *Information Sciences and Systems, 43rd Annual Conference on (CISS)*, Baltimore, USA, Mar. 2009.
[8] 3GPP TS 36.212 V8.8.0, "Evolved universal terrestrial radio access (E-UTRA): Multiplexing and channel coding," Dec. 2009.
[9] S. N. Donthi and N. B. Mehta, "An accurate model for EESM and its application to analysis of CQI feedback schemes and scheduling in LTE," *Wireless Communications, IEEE Transactions on*, vol. 10, no. 10, pp. 3436–3448, Oct. 2011.
[10] C. Mehlführer, M. Wrulich, J. C. Ikuno, D. Bosanska, and M. Rupp, "Simulating the Long Term Evolution physical layer," in *Proc. of the 17th European Signal Processing Conference (EUSIPCO)*, Glasgow, Scotland, Aug. 2009.
[11] 3GPP TS 36.213 V8.8.0, "Evolved universal terrestrial radio access (E-UTRA): Physical layer procedures," Sep. 2009.
[12] C. Liu, A. Schmeink, and R. Mathar, "Dual optimal resource allocation for heterogeneous transmission in OFDMA systems," in *Globecom, IEEE*, Honolulu, Hawaii, USA, Dec. 2009.
[13] X. Xu, G. Kutrolli, and R. Mathar, "Autonomous downlink power control for lte femtocells based on channel quality indicator," in *IEEE 24th International Symposium on Personal, Indoor and Mobile Radio Communications (PIMRC)*, London, UK, Sep 2013.
[14] T. Zahir, K. Arshad, A. Nakata, and K. Moessner, "Interference management in femtocells," *Communications Surveys Tutorials, IEEE*, vol. 15, no. 1, pp. 293–311, 2013.
[15] 3GPP R4-092042, "Simulation assumptions and parameters for FDD HeNB RF requirements," Alcatel-Lucent, picoChip Designs, Vodafone.
[16] K. E. Baddour and N. C. Beaulieu, "Autoregressive modeling for fading channel simulation," *Wireless Communications, IEEE Transactions on*, vol. 4, no. 4, pp. 1650–1662, Jul. 2005.